THEORY OF BLIND NAVIGATION BY DYNAMICAL MEASUREMENTS

J. J. Gilvarry, S. H. Browne and I. K. Williams

P-121

December 29, 1949

The RAND Corporation
1700 MAIN ST. • SANTA MONICA • CALIFORNIA

31

THEORY OF BLIND NAVIGATION BY DYNAMICAL MEASUREMENTS

J. J. Gilvarry, S. H. Browne and I. K. Williams

The RAND Corporation, Santa Monica, California

- - - - - - - - - - - - - - - - -

The differential equation is considered which determines the position of a vehicle from dynamical measurements of the non-gravitational acceleration $\underset{\sim}{b}$ made internally. Three linear approximations to the gravitational field $\underset{\sim}{g}(\underset{\sim}{r})$ of the earth, which lead to explicit solutions of this equation, are considered and their limitations are discussed. An interval-wise solution (linear continuation) for trajectories of extended range is described, which is based on such linear approximations and has definite advantages in this application. The theory is applied to the trajectory of the German A10 vehicle.

- - - - - - - - - - - - - - - - -

Current developments in rocket and jet propulsion have made blind navigation a matter of practical importance. This paper discusses the theory of blind navigation by means of dynamical measurements (measurements of forces or accelerations) made on a proof body in a reference frame internal to a vehicle. Instrumentally, such measurements are made by an accelerometer in a reference frame provided by gyroscopic or other means. A navigation system essentially of the type considered was used in the German V2. In the following discussion, the vehicle will be idealized as a windowless box.

Under the assumption of local uniformity of the gravitational field, the information derivable from the accelerometer is limited[1] by the applicability

- -

(1) J. J. Gilvarry, Phys. Rev. 73, 1409 (1948). A misprint exists in this letter; in the first line of the second column of p. 1410, delete "vertically."

- -

of Einstein's equivalence principle. In fact, an application of this principle was pointed out by the investigator(2) who built the first (consciously-designed)

(2) F. W. Lanchester, Proc. Phys. Soc. 19, 691 (1905).

accelerometer.

1. The g-Correction Equation.

The accelerometer reference frame Q will be taken non-rotating for convenience, with origin at a point Q in the box. If $\underset{\sim}{R}$ is the radius vector of the point Q referred to an inertial reference frame O, then the acceleration $d^2\underset{\sim}{R}/dt^2$ of this point must consist of two parts: a part $\underset{\sim}{g}$ due to the local gravitational acceleration in space, and a part $\underset{\sim}{b}$ due to the operation of non-gravitational forces. Thus one has

$$d^2\underset{\sim}{R}/dt^2 = \underset{\sim}{g} + \underset{\sim}{b}. \tag{1}$$

rho

If $\underset{\sim}{\rho}$ is the radius vector in the frame Q of the proof body and m is its mass, the equation of motion of this body in the inertial frame O is

$$d^2(\underset{\sim}{R}+\underset{\sim}{\rho})/dt^2 = \underset{\sim}{g} + \underset{\sim}{L}/m, \tag{2}$$

where $\underset{\sim}{L}$ is the force on the proof body linking it to the box. Subtraction of (1) from (2) yields

$$d^2\underset{\sim}{\rho}/dt^2 - \underset{\sim}{L}/m = -\underset{\sim}{b} \tag{3}$$

for the equation of motion of the proof body in the observer's frame Q. If the quantity on the left-hand side in Eq. (3) is defined as the reading of the accelerometer, it follows that an accelerometer reads the negative of the acceleration of the origin of its associated reference frame due to non-gravitational forces. From the method of derivation, it is clear that Eq. (3) holds independently of variation of mass, rotation, or non-rigidity of the box.

In Eq. (1) only the term $\underset{\sim}{b}$ is susceptible to physical measurement in the box, and the observer can integrate the differential equation to yield his position vector $\mathbf{R}(t)$ only if he knows the functional form of $\mathbf{g}$ in its dependence on position coordinates and also the initial position and velocity of the box. When the term $\mathbf{g}$ is replaced by the function specifying its dependence on position coordinates in space, and the term $\mathbf{b}$ is considered a function $\mathbf{b}(t)$ of time, Eq. (1) will be referred to as the g-correction equation.

For motion of the box in the earth's neighborhood, the inertial frame O can be taken as approximately geocentric. It is convenient to select an initial point O_o with radius vector $\mathbf{R}_o$ which, in general, is outside the earth's surface and on the curve of motion C (Fig. 1). The gravitational field corresponding to a spherical earth is

$$\mathbf{g} = -g_o (R_o^2/R^3)\mathbf{R}, \tag{4}$$

if g_o is the value of g at O_o. The g-correction equation then becomes

$$d^2\mathbf{R}/dt^2 + g_o(R_o^2/R^3)\mathbf{R} = \mathbf{b}(t). \tag{5}$$

IG1 The sphere S_o (Fig. 1) through O_o and concentric with the earth will be referred to as the reference sphere. For an initial point on the actual (approximately spheroidal) earth, the radius and surface gravitation of the reference sphere can be taken as the mean radius R_e and mean gravitational acceleration g_e over the earth's surface, which are defined(4) in first approximation by

$$R_e = (2/3)R_{eq} + (1/3)R_{pol}, \tag{6a}$$

$$g_e = (2/3)g_{eq} + (1/3)g_{pol}, \tag{6b}$$

---

(4) G. G. Stokes, Camb. and Dubl. Math. Jour. 4, 194 (1849); Trans. Camb. Phil. Soc. 8, 672 (1849); also Mathematical and Physical Papers (Cambridge University Press, Cambridge, 1883), Vol. II, p. 104.

---

where R_{eq} and R_{pol} are the equatorial and polar radii respectively of the earth, and g_{eq} and g_{pol} are the corresponding gravitational accelerations. The radius R_e is, in first approximation, equal to the radius of the earth's sphere of equal volume, and defines an equivalent sphere S_e (Fig. 1) with surface gravity g_e for the earth.[5] Eq. (5) is valid in a geocentric frame O' fixed in the rotating

(5) The equality of volumes follows on the assumption that squares and higher powers of the ellipticity $e = (R_{eq} - R_{pol})/R_{eq}$ are negligible compared to unity. If the density of the earth's crust is assumed constant, R_e is likewise the radius of the earth's sphere of equivalent mass. Hence, Eq. (4) with $R_o = R_e$ and $g_o = g_e$ yields the correct asymptotic value GM/R^2 (G = gravitational constant, M = mass of the earth) of g at large distances from the earth.

earth if the centrifugal and Coriolis accelerations (and the latitude-dependent component of $\underset{\sim}{g}$) can be neglected.[6]

(6) Eq. (5) likewise ignores a slight perturbation due to lunar and solar attraction (similar in origin to the perturbations producing tides). The corresponding effect for artillery shells is discussed in F. R. Moulton, New Methods in Exterior Ballistics (University of Chicago Press, Chicago, 1926), p. 19.

Let a Cartesian frame O_o (Fig. 1) be defined with origin at the initial point of motion, such that the z-axis is vertical, the x-axis is horizontal in the plane determined by the z-axis and the initial velocity vector $\underset{\sim}{v}_o$, and the y-axis is selected to make the frame right-handed. It will be assumed for simplicity in what follows that the initial velocity $\underset{\sim}{v}_o$ is non-vanishing unless otherwise stated (and hence the convention above defines the direction of the x-axis except when the initial velocity is in the vertical direction). If $\underset{\sim}{r} = x\underset{\sim}{i} + y\underset{\sim}{j} + z\underset{\sim}{k}$ is the radius vector of the box in the frame O_o, Eq. (5) becomes

$$d^2\underset{\sim}{r}/dt^2 + \omega_o^2 (R_o/R)^3 (R_o\underset{\sim}{k} + \underset{\sim}{r}) = \underset{\sim}{b}(t). \qquad (7)$$

omega where the parameter ω_o is defined by

$$\omega_o = (g_o/R_o)^{1/2}. \qquad (8)$$

and

$$R = [x^2 + y^2 + (z + R_o)^2]^{1/2}; \qquad (9)$$

with $\underset{\sim}{b} = b_x\underset{\sim}{i} + b_y\underset{\sim}{j} + b_z\underset{\sim}{k}$. The initial conditions are $\underset{\sim}{r}_o = 0$ and $\underset{\sim}{v}_o = v_{x,o}\underset{\sim}{i} + v_{z,o}\underset{\sim}{k}$.

Eq. (7) can be formulated as an integral equation

tau $$\underset{\sim}{r} = \underset{\sim}{v}_o t + \int_o^t (t-\tau)[\underset{\sim}{b}(\tau) + \underset{\sim}{g}(\underset{\sim}{r})]\,d\tau, \qquad (10)$$

in which $\mathbf{g}(\mathbf{r})$ is $\mathbf{g}$ of (4) with its dependence on components of $\mathbf{r}$ represented

tau symbolically, and the cubature operator $\int_0^t (t - \tau)d\tau$ performs the operation of double integration with respect to time (as integration by parts verifies). From

'IG 2 the standpoint of an automatic computer in the box, the sequence of operations shown diagramatically in Fig. 2 yields the position vector $\mathbf{r}(t)$ from $\mathbf{b}(t)$ (the

delta initial velocity $\mathbf{v}_0$ has been put in symbolically by means of the Dirac δ-function, $\delta(t)$, which is singular at $t = 0$).

From the standpoint of determining $\mathbf{r}(t)$ as a closed solution in the time, Eq. (7) poses serious difficulties since $\mathbf{b}(t)$ is an arbitrary function of time and the equation is non-linear in $\mathbf{r}$. In the general case, integrals of energy and angular momentum cannot be found except as purely formal expressions. Hence, the classical method of using integrals of the motion to reduce the order of the component differential equations is not possible in general. Exact solutions in some particular cases are available; if $\mathbf{b}$ is zero, for example, Eq. (7) reduces to the differential equation of an elliptical free-flight trajectory. In practical cases, however, $\mathbf{b}$ and $\mathbf{g}$ are of comparable magnitude over the trajectory as a whole (see Fig. 4), so that perturbation methods are not generally useful. Resort can be made to various numerical and iterative methods. A difference method due to Hartree,[7] which avoids intermediate computation of the velocities, can be

(7) D. R. Hartree, Mem. Manch. Lit. Phil. Soc. 77, 91 (1932).

mentioned. The integral equation (10) can be identified in coordinate formulation with a system of non-linear Volterra integral equations of the second kind[8] to

(8) V. Volterra, Leçons sur les Equations Intégrales (Gauthier-Villars, Paris, 1913) p. 90.

yield a general solution by iteration. Although iterative solutions have obvious limitations, a solution of this type has been applied [9] as a computational

(9) E. T. Benedikt, Phys. Rev. 74, 1213(A) (1948).

method for specific $\mathbf{b}(t)$.

In the practical problem of computer design, the non-linear $\mathbf{g}$-term of Eq. (7) presents design complications. Furthermore, a suitable approximation for $\mathbf{g}$ may be sufficient on trajectories of restricted range, or when the motion is constrained to a particular surface (see Sec. 2). The simplest such approximation consists in replacing $\mathbf{g}$ by its constant value $-g_o\mathbf{k}$ at O_o, which yields the zero-order solution

tau

$$\mathbf{r} = \mathbf{v}_o t - (g_o t^2/2)\mathbf{k} + \int_0^t (t-\tau)\mathbf{b}(\tau)\,d\tau, \qquad (11)$$

valid in a restricted neighborhood of the origin. The remainder of this paper will consider the problem of replacing $\mathbf{g}$ by linear approximations. These linear approximations will be made the basis of an interval-wise solution having certain advantages.

2. The Spherical Solution.

The g-correction equation (7) has a simple and exact solution when the vehicle is constrained to move on the surface of a sphere concentric with the earth, and the corresponding solution will be referred to as a spherical solution. The sphere of motion will be taken as the reference sphere of radius R_o, on which the outward-drawn unit normal is $\mathbf{R}/R_o$ or $\mathbf{k} + \mathbf{r}/R_o$. The condition on $\mathbf{b}$ for motion on S_o is

$$\mathbf{b}\cdot(R_o\mathbf{k} + \mathbf{r}) = g_o R_o^2/R - v^2, \qquad (12)$$

which is necessary and sufficient if the initial velocity vector is tangent to S_o at O_o ($\mathbf{v}_o = v_o\mathbf{i}$). Physically, Eq. (12) states (when divided by R) that the radial component of $\mathbf{b}$ equals the gravitational acceleration less the centrifugal acceleration on a sphere of radius R. In practice, the condition (12) can be met by means of an altimeter (of atmospheric-pressure or radar type) used to control independently the altitude of the vehicle relative to the earth. The field $\mathbf{g}_s$ on the surface of S_o is

omega

$$\mathbf{g}_s = -g_o\mathbf{k} - \omega_o^2\mathbf{r}, \qquad (13)$$

which will be referred to as the spherical field.

The g-correction equation in the spherical case is

omega

$$d^2 \underset{\sim}{r}/dt^2 + \omega_0^2 \underset{\sim}{r} = \underset{\sim}{b} - g_0 \underset{\sim}{k}. \tag{14}$$

The solution of Eq. (14) subject to the condition (12) on $\underset{\sim}{b}$ is

tau

$$\underset{\sim}{r} = [(\sin \omega_0 t)/\omega_0] \underset{\sim}{v}_0 - [2 R_0 \sin^2 \omega_0 t/2] \underset{\sim}{k} + (1/\omega_0) \int_0^t \underset{\sim}{b}(\tau) \sin \omega_0 (t-\tau)\, d\tau, \tag{15}$$

with the restriction that $\underset{\sim}{v}_0 = v_0 \underset{\sim}{i}$. If the sine functions appearing in the spherical solution are replaced by the leading terms of their Taylor expansions, the spherical solution (15) reduces to the zero-order solution (11).

As a trivial example of the spherical solution, consider a box moving on the surface of the reference sphere S_0 and such that $\underset{\sim}{b} = 0$. From Eq. (12), the speed $v_{s,0}$ is a constant

$$v_{s,0} = (g_0 R_0)^{1/2}. \tag{16}$$

Eq. (15) in this case corresponds to a circle of radius R_0 described with the constant angular velocity ω_0 and the period

π pi

$$T_0 = 2\pi (R_0/g_0)^{1/2}, \tag{17}$$

which is approximately 84.4 min. for an origin on the equivalent sphere S_e. Hence, this special case corresponds physically to the motion of a satellite around the earth in a circular orbit, and the speed $v_{s,0}$ will be referred to as the satellite speed corresponding to the radius R_0.

When the constraining condition (12) is not satisfied exactly at all times, the altitude,

$$h = R - R_0, \tag{18}$$

of the vehicle relative to the reference sphere S_0 is non-vanishing, and the

δ delta

spherical solution (15) yields a corresponding error. If $\delta_s \underset{\sim}{r}$ is the true solution of Eq. (7) less the spherical solution of (15) for a given $\mathbf{b}$, then one has

omega
delta
xi

$$d^2\delta_s\mathbf{r}/dt^2 + \omega_0^2\delta_s\mathbf{r} = g_0\,\xi\,(\mathbf{k} + \mathbf{r}/R_0), \tag{19}$$

where the error parameter ξ is defined by

$$\xi = 1 - (R_0/R)^3 \sim 3h/R_0, \tag{20}$$

and the approximation indicated is valid for $h \ll R_0$. The quantity $\xi(\mathbf{k} + \mathbf{r}/R_0)$ is the gradient of a harmonic function, and hence its magnitude assumes a maximum value on the boundary of any closed region of space (not including the center of the earth) considered. Thus, if a uniform bound H on the absolute value of h is known, then

$$M = (1 - H/R_0)^{-2} - (1 - H/R_0) \sim 3H/R_0 \tag{21}$$

is a uniform bound on $|\xi(\mathbf{k} + \mathbf{r}/R)|$ for $H < R_0$, and hence one can show that

$$|\delta_s\mathbf{r}| \le 2g_0 M \sin^2\omega_0 t/2, \qquad (t \le T_0/2), \tag{22}$$

if no error exists in the knowledge of initial conditions (the direction of $\mathbf{v}_0$ is now unrestricted). Since $|\delta_s\mathbf{r}|$ vanishes as $M \rightarrow 0$ (or $H \rightarrow 0$), the spherical solution (15) is a valid approximation in the large (or "on the average") for motion which is closely spherical, within the limitations of (22) or a closer error bound.

Over a trajectory of extended range, the spherical solution is not useful if significant systematic variations of altitude exist. The difficulty usually cannot be avoided by taking an average R corresponding to an average altitude in the $\mathbf{g}$-term of Eq. (7); this point can be illustrated by an example. Fig. 3 shows the trajectory (solid curve) of the German A10 vehicle(10)(11), which is

/G 3

- -

(10) W.G.A. Perring, J. Roy. Aero. Soc. 50, 483 (1946).

(11) J.M.J. Kooy and J.W.H. Uytenbogaart, Ballistics of the Future (McGraw-Hill Book Co., Inc., New York, 1946), p. 399.

- -

FIG 4

extreme in its altitude variation (185 mi.), and Fig. 4 shows the non-gravitational accelerations[12] b_x and b_z for this vehicle as a function of time. For this

---

(12) Only a limited amount of information is available on the A10 (this vehicle was proposed but never built, and was to consist essentially of a winged V2 equipped with a booster rocket). The trajectory of Fig. 3 fits the A10 as closely as the available information permits. The quantities b_x and b_z were determined by differentiation from the assumed trajectory. Of the peaks in each curve of Fig. 4, the first two correspond to release of the booster and power cut-off in that order, and the ones at 560 seconds correspond to re-entry into appreciable atmosphere. Rotation of the earth and latitude variation of g have been completely neglected in the data of Figs. 3 and 4.

---

trajectory, a solution of the g-correction equation is shown in Fig. 3 (dashed curve) which corresponds to an average altitude of 16.9 mi.(i.e. R was taken as R_e + 16.9 mi. in the $\mathbf{g}$-term of Eq. (7)). This particular average-altitude solution yields a negligible error at the terminal point of the motion but defines a trajectory passing under the earth's surface.

3. The Linearized Approximation.

It is clear from the preceding discussion that the essential problem in connection with the g-correction equation exists when significant variations in altitude above the earth occur. This section discusses an approximate analytic solution which is superior to the zero-order approximation (11) when variations in altitude above the earth occur.

The field $\mathbf{g}(\mathbf{r})$ of (4) can be expanded about the origin O_o to yield

omega

$$\mathbf{g}(\mathbf{r}) = -g_0\mathbf{k} - \omega_0^2[\mathbf{r} - 3(\mathbf{k}\cdot\mathbf{r})\mathbf{k}] - (3\omega_0^2/2R_0)\{[5(\mathbf{k}\cdot\mathbf{r})^2 - r^2]\mathbf{k} - 2(\mathbf{k}\cdot\mathbf{r})\mathbf{r}\} + \cdots \quad (23)$$

If only linear terms are retained in the Taylor expansion (23), the corresponding field $\mathbf{g}_L$, defined by

$$\mathbf{g}_L(\mathbf{r}) = -g_0\mathbf{k} - \omega_0^2[x\mathbf{i} + y\mathbf{j} - 2z\mathbf{k}], \quad (24)$$

will be referred to as the linearized field. Under this approximation for $\mathbf{g}$, the coordinate formulation of the g-correction equation becomes

omega

$$\ddot{x} + \omega_0^2 x = b_x , \tag{25a}$$

$$\ddot{z} - 2\omega_0^2 z = b_z - g_0 , \tag{25b}$$

with the y-equation symmetric to that in x. These differential equations, which are valid in some neighborhood of the origin, will be referred to as the linearized equations.

The linearized solution will be taken as

tau

$$x = (v_{x,o}/\omega_o) \sin \omega_o t + (1/\omega_o)\int_0^t b_x(\tau) \sin \omega_o (t-\tau) d\tau , \tag{26a}$$

$$y = (1/\omega_o)\int_0^t b_y(\tau) \sin \omega_o (t-\tau) d\tau , \tag{26b}$$

$$z = (v_{z,o}/2^{1/2}\omega_o) \sinh 2^{1/2}\omega_o t - R_o \sinh^2 \omega_o t/2^{1/2}$$
$$+ (1/2^{1/2}\omega_o)\int_0^t b_z(\tau) \sinh 2^{1/2}\omega_o (t-\tau) d\tau . \tag{26c}$$

The case of a flat earth corresponds to $R_o \rightarrow \infty$, or equivalently $\omega_o \rightarrow 0$. Eqs. (26) reduce directly to the zero-order solution (11) for a flat earth as $\omega_o \rightarrow 0$ if note is taken of the limits $(\sin u)/u \rightarrow 1$, $(\sinh u)/u \rightarrow 1$ as $u \rightarrow 0$.

The linearized field $\underset{\sim}{g}_L$ is symmetric about the z-axis. In the meridian x,z plane, the equipotentials of the linearized field are defined by

$$(z - R_o/2)^2 - x^2/2 = const. , \tag{27}$$

and the field lines are given by

$$x^2 (z - R_o/2) = const. \tag{28}$$

Hence, the equipotentials form in the x,z plane a family of concentric hyperbolas and their conjugates asymptotic to the lines $x^2 = 2(z - R_o/2)^2$ through the center of symmetry $(0, R_o/2)$ of the field. The linearized field diagram is shown in Fig. 5 (solid curves, field lines indicated by arrows). On the horizontal plane $z = R_o/2$, the z-component of the linearized field vanishes and above this plane the field becomes repulsive. The field diagram of Fig. 5 yields a qualitative index of the extent of the neighborhood of the origin in which the linearized equations provide a practical approximation.

In discussing the degree of approximation of the linearized solution, the error vector $\delta_L \underset{\sim}{r}$ with components $\delta_L x$, $\delta_L y$, $\delta_L z$ will represent the true less the linearized solution. By subtracting the linearized equations (25) from the corresponding component equations of (7), one obtains (omitting the equation for $\delta_L y$ symmetric to that in $\delta_L x$)

delta

omega

xi

zeta

$$d^2 \delta_L x/dt^2 + \omega_0^2 \delta_L x = \omega_0^2 \xi x, \tag{29a}$$

$$d^2 \delta_L z/dt^2 - 2\omega_0^2 \delta_L z = \omega_0^2 \zeta R_0, \tag{29b}$$

where ξ is given by (20) and the error parameter ζ is defined by

$$\zeta = 1 - 2z/R_0 - (1 + z/R_0)(R_0/R)^3 \sim -3z/R_0 . \tag{30}$$

Physically, the right-hand sides of Eqs. (29a) and (29b) are the accelerations neglected by $\underset{\sim}{g}_L$ on the x- and z-axes respectively. If bounds max $(|\xi x|)$ and max $(|\zeta R_0|)$ are known from sources other than the linearized solution itself, then one has

$$|\delta_L x| \leq 2 \max(|\xi x|) \sin^2 \omega_0 t/2 ; \qquad (t \leq T_0/2); \tag{31a}$$

$$|\delta_L z| \leq \max(|\zeta R_0|) \sinh^2 \omega_0 t/2^{1/2} . \tag{31b}$$

Both ξx and ζR_0 are harmonic functions, so their maximum and minimum values must be on the boundary of any closed region of space (not containing the center of the earth) considered.

It follows from (29) that the linearized x- and z-solutions are exact for motion of the box on surfaces such that $\xi x = 0$ and $\zeta = 0$ respectively. If one disregards the trivial locus represented by the z-axis, the reference sphere $R = R_0$ is (from Eq. (20)) the surface of zero error $\xi = 0$ for the linearized x-solution (and for the linearized y-solution, by symmetry). The surface defined zeta

by $\zeta = 0$ is a surface of revolution about the z-axis, and consists of two sheets intersecting the origin O_o which are shown (dashed curves) in x, z coordinates on the linearized field diagram of Fig. 5. The upper open branch in Fig. 5 is asymptotic to the line $z = R_o/2$, and the upper and lower branches behave in the neighborhood of the origin O_o as segments (for x positive) of the two straight lines $x^2 = 2z^2$. It is seen that no surface exists on which all components of the linearized solution are exact.

FIG 5

delta

The leading term of the Taylor expansion of the error $\delta_L \underset{\sim}{r}$ is given by

omega

$$\delta_L \underset{\sim}{r} = R_o \left[2 v_{x,o} v_{z,o} \underset{\sim}{i} + (v_{x,o}^2 - 2 v_{z,o}^2) \underset{\sim}{k} \right] (\omega_o t)^4 / 4 v_{e,o}^2 + \cdots , \tag{32}$$

where $v_{e,o}$ is the escape (or parabolic) speed

$$v_{e,o} = (2 g_o R_o)^{1/2} . \tag{33}$$

The leading terms of $\delta_L x$ and $\delta_L z$ vanish for motions initially tangent to the corresponding surfaces of zero error, respectively, and hence never vanish simultaneously. For $\underset{\sim}{v}_o \neq 0$ the absolute error $|\delta_L \underset{\sim}{r}| = \underline{O}(t^4)$ is never of order higher than t^4, and thus the Taylor expansion of the linearized solution agrees with the true Taylor expansion of $\underset{\sim}{r}$ through terms of order t^3, as compared to the zero-order solution (11), which agrees through terms of order t^2. Since $s = \underline{O}(t)$ when $\underset{\sim}{v}_o \neq 0$, the linearized trajectory has contact of order not less than the third with the actual trajectory at the origin, and hence the linearized solution is essentially an osculating approximation.

For the case $\underset{\sim}{b} = 0$ (ballistic trajectory), the linearized trajectory can be compared with the exact solution representing an ellipse in space and with the corresponding parabola. It is convenient to introduce the dimensionless parameters

mu
sigma

$$\mu_o = v_{x,o} / (g_o R_o)^{1/2} , \qquad \sigma_o = v_{z,o} / (2 g_o R_o)^{1/2} , \tag{34}$$

for the initial velocities, where the denominators in μ_o and σ_o are respectively

sigma
mu

the satellite speed $v_{s,o}$ of (16) and the escape speed $v_{e,o}$ of (33) (one has $\sigma_o^2 + \mu_o^2/2 \leq 1$ if $v_o \leq v_{e,o}$). The linearized solution for $\underset{\sim}{b} = 0$ can be written

omega
tau

$$x = R_o \mu_o \sin \omega_o t, \tag{35a}$$

$$z = (R_o/2)\left[1 - (1 - 4\sigma_o^2)^{1/2} \cosh\left(t/\tau_o - \tanh^{-1} 2\sigma_o\right)\right], \tag{35b}$$

in which the parameter τ_o is

$$\tau_o = 1/2^{1/2} \omega_o, \tag{36}$$

and it is assumed that $|\sigma_o| < 1/2$. If $\sigma_o = 1/2$, the z-solution becomes

$$z = (R_o/2)\left[1 - e^{-t/\tau_o}\right], \tag{37}$$

and hence the trajectory defined by the linearized solution approaches the plane $z = R_o/2$ asymptotically as $t \to \infty$. The time constant τ_o for z to reach the fraction $1 - 1/e$ of its asymptotic value in this case is approximately 9.5 min. for an initial point O_o on the surface of the equivalent sphere S_e. For $\sigma_o > 1/2$, the linearized trajectory crosses the plane $z = R_o/2$ and is unbounded in z; thus the linearized approximation implies an escape speed $v_{e,o}/2$ which is one-half the true value (33) on an inverse-square field. For $0 < \sigma_o < 1/2$, the time of flight t_f corresponding to intersection with the x,y plane,

$$t_f = 2\tau_o \tanh^{-1} 2\sigma_o, \tag{38}$$

FIG 6

is compared in Fig. 6 with the corresponding time of flight $4\sigma_o \tau_o$ for a parabola, and, for a few values of μ_o, with the corresponding time of flight on an inverse-square field.

In Fig. 7, linearized trajectories from Eqs. (35) are shown (solid curves) in two families ($\sigma_o = 0.3$ and $\mu_o = 0.2$). From Eq. (35a) one notes that all the linearized trajectories for $\underset{\sim}{b} = 0$ intersect the z-axis at time $t = T_o/2$. For σ_o small and thus t_f small relative to $T_o/2$ (as in the family $\sigma_o = 0.3$), this intersection point is far below the x,y plane, and above this plane, the linearized trajectories show a fairly close resemblance in the large to the corresponding

FIG 7

ellipses (dashed curves). The intersection with the z-axis is at the origin O_o

pi
sigma

for $t_f = T_o/2$, which fixes a critical value $(\tanh \pi/2^{1/2})/2 = 0.488$ of σ_o at which the upward and downward branches of the linearized trajectory above the x,y plane coincide. It is clear that for σ_o close to 1/2, the linearized trajectories for $\mathbf{b} = 0$ are a very poor approximation in the large to the corresponding ellipses, although they are superior to the corresponding parabolas (dot-and-dashed curves) in a neighborhood of the origin.

4. The Quasilinear Approximation.

The linearized approximation is based on the assumption that the gravitational acceleration $\mathbf{g}$ is a slowly varying function of position. This section discusses a linear approximation based on the additional assumptions that the radius of curvature of the trajectory is large and is a slowly varying function. The approximation will be referred to as the quasilinear approximation. For simplicity, only motion confined to the vertical x,z plane will be considered.

If the curve of motion is an analytic curve at the origin O_o, the radius vector $\mathbf{r}$ to a point on the curve can be expanded in the series[13]

(13) W. C. Graustein, Differential Geometry (Macmillan Co., New York, 1947), p. 39.

alpha
beta
rho

$$\mathbf{r} = \boldsymbol{\alpha}_o s + (\boldsymbol{\beta}_o/2\rho_o)s^2 + \cdots, \qquad (39)$$

where s is the arc length on the curve, $\boldsymbol{\alpha}_o$ and $\boldsymbol{\beta}_o$ are the unit tangent and unit principal normal at O_o respectively, and ρ_o is the radius of curvature at O_o. The terms of order s^3 and higher in (39) involve first and higher derivatives with respect to s and powers above the first of the curvature $1/\rho$. If the series (39) for $\mathbf{r}$ is substituted in (23) for $\mathbf{g}(\mathbf{r})$, one obtains

omega

$$\mathbf{g}(\mathbf{r}) = -g_o\mathbf{k} - \omega_o^2[\boldsymbol{\alpha}_o - 3(\boldsymbol{\alpha}_o\cdot\mathbf{k})\mathbf{k}]s$$
$$- \frac{3\omega_o^2}{2}\left\{\frac{\boldsymbol{\beta}_o/3 - (\boldsymbol{\beta}_o\cdot\mathbf{k})\mathbf{k}}{\rho_o} + \frac{[5(\boldsymbol{\alpha}_o\cdot\mathbf{k})^2 - 1]\mathbf{k} - 2(\boldsymbol{\alpha}_o\cdot\mathbf{k})\boldsymbol{\alpha}_o}{R_o}\right\}s^2 + \cdots, \qquad (40$$

where the terms given explicitly represent $\underset{\sim}{g}$ under the assumption that terms of order s^3 or higher are negligible. Consider the canonical coordinates x_1

alpha
beta

and x_2 (defined as coordinates in the direction of $\underset{\sim}{\alpha}_o$ and $\underset{\sim}{\beta}_o$ respectively) of the curve at the origin. The coordinates x_1 and x_2 are given in terms of x and z by

$$\begin{Bmatrix} x_1 \\ x_2 \end{Bmatrix} = \begin{bmatrix} \alpha_{x,o} & \alpha_{z,o} \\ \beta_{x,o} & \beta_{z,o} \end{bmatrix} \begin{Bmatrix} x \\ z \end{Bmatrix}, \qquad (41)$$

where the elements of the direction-cosine matrix are components of $\underset{\sim}{\alpha}_o$ and $\underset{\sim}{\beta}_o$; these coordinates are likewise given by

rho

$$x_1 = s, \qquad x_2 = s^2/2\rho_o, \qquad (42)$$

from (39) under the approximation that terms of order s^3 or higher are negligible. By comparison of (41) and (42), one has the approximation

$$s = \alpha_{x,o}\, x + \alpha_{z,o}\, z, \qquad (43a)$$
$$s^2 = 2\rho_o[\beta_{x,o}\, x + \beta_{z,o}\, z], \qquad (43b)$$

which expresses both s and s^2 linearly in terms of x and z. Under the substitution (43), the terms given explicitly in (40) yield the quasilinear field $\underset{\sim}{g}$ defined (in matrix notation) by

omega

$$\underset{\sim}{g}_Q = -\begin{Bmatrix} 0 \\ g_o \end{Bmatrix} - \omega_o^2 \underset{\sim}{A}_o \begin{Bmatrix} x \\ z \end{Bmatrix} \qquad (44)$$

where the coefficient matrix $\underset{\sim}{A}_o$ is

$$\underset{\sim}{A}_o = \begin{bmatrix} 1 - 6\alpha_{x,o}\alpha_{z,o}\beta_{x,o}\rho_o/R_o & 6\alpha_{x,o}\alpha_{z,o}\beta_{z,o}\rho_o/R_o \\ 3\beta_{x,o}(3\alpha_{z,o}^2 - 1)\rho_o/R_o & -2 + 3\beta_{z,o}(3\alpha_{z,o}^2 - 1)\rho_o/R_o \end{bmatrix}. \qquad (45)$$

The parameters entering the coefficient matrix $\underset{\sim}{A}_o$ can be evaluated directly from the initial conditions of the motion. From standard formulae(13), one has

cross

$$\underset{\sim}{\alpha}_o = \frac{\underset{\sim}{V}_o}{V_o}, \qquad \underset{\sim}{\beta}_o = \frac{\underset{\sim}{V}_o \times (\underset{\sim}{b}_o - g_o \underset{\sim}{k})}{|\underset{\sim}{V}_o \times (\underset{\sim}{b}_o - g_o \underset{\sim}{k})|} \times \frac{\underset{\sim}{V}_o}{V_o}, \qquad (46)$$

and

rho

cross

$$\rho_0 = v_0^{\,3} / |\underset{\sim}{v}_0 \times (\underset{\sim}{b}_0 - g_0 \underset{\sim}{k})| , \tag{47}$$

where $\underset{\sim}{b}_0$ is the initial value of $\underset{\sim}{b}$ and it is assumed that $\underset{\sim}{v}_0$ is non-vanishing. The corresponding quasilinear equations of motion are given by

omega

$$\begin{Bmatrix} \ddot{x} \\ \ddot{z} \end{Bmatrix} + \omega_0^2 \underset{\sim}{A}_0 \begin{Bmatrix} x \\ z \end{Bmatrix} = \begin{Bmatrix} b_x \\ b_z - g_0 \end{Bmatrix} . \tag{48}$$

Solutions of the system (48) can be obtained directly by the use of the Laplace transform.

The quasilinear approximation represented by Eqs. (48) yields a transition from the linearized approximation (25) to the spherical approximation (14). The linearized equations assume that terms of the type $(x/R_0)^2$ in the Taylor expansion of $\underset{\sim}{g}$ are negligible compared to terms of type x/R_0, which is equivalent to assuming $(s/R_0)^2 << s/R_0$. From Eqs. (43) this condition requires that $\rho_0 << R_0$, and one notes that Eqs. (48) reduce to the linearized equations (25) when $\rho_0 \rightarrow 0$. The spherical solution (15) for motion in the x,z plane presupposes $\underset{\sim}{\alpha}_0 = i$ and $\underset{\sim}{\beta}_0 = -\underset{\sim}{k}$ at the origin; if note is taken of the constraining condition (12) on $\underset{\sim}{b}_0$, Eq. (47) yields $\rho_0 = R_0$. With these values of the parameters, Eqs. (48) reduce directly to the spherical equation (14) of motion.

alpha

beta

Since the terms in the Taylor expansion of $\underset{\sim}{g}$ neglected by $\underset{\sim}{g}_Q$ are of order s^3, and $s = \underline{O}(t)$ when $\underset{\sim}{v}_0 \neq 0$, it follows that the absolute error $|\delta_Q \underset{\sim}{r}|$ of the quasilinear solution is such that $|\delta_Q \underset{\sim}{r}| = \underline{O}(t^5)$ in general. Thus, the Taylor expansion of the quasilinear solution agrees with the true Taylor expansion of $\underset{\sim}{r}$ through terms of order t^4 in general, as compared to the linearized solution (26), which agrees through terms of order t^3 at most. The quasilinear trajectory has contact of order not less than the fourth with the actual trajectory at the origin, and accordingly is an osculating approximation in general.

delta

One can define error parameters for the quasilinear equations analogous to xi zeta ξ and ζ in the linearized case, which fix surfaces of zero error for the component equations of (48). By this means one can show that the surfaces of zero error for both components coincide, and the quasilinear system (48) is exact if and only if the motion is constrained to the reference sphere S_o (condition (12) holds), in which case the quasilinear system reduces to the spherical equation (14). rho When $\rho_o \sim R_o$, the surfaces of zero error for both components are nearly in coincidence, and the quasilinear solution provides an approximation which is markedly superior to the linearized. When ρ_o is small relative to R_o, the quasilinear trajectory differs only slightly from the linearized, and may yield only a small margin of gain. These results are illustrated by Fig. 8, which FIG 8 compares the quasilinear trajectories for the ballistic case ($b = 0$) with the sigma corresponding ellipses and linearized trajectories when $\sigma_o = 0$.

In passing, it can be noted that generalization of this quasilinear approximation to three dimensions is easily made (by assuming that the torsion of the curve of motion is likewise a slowly varying function).

5. <u>Linear Continuation</u>.

When significant variations of altitude above the earth occur on a trajectory of extended range, it is clear that none of the linear approximations given for $g(r)$ are satisfactory in the large. In this case, the g-correction equation (7) can always be solved by a step-by-step procedure in which the non-linear gravitational term over any interval of time is replaced by a constant value corresponding to the interval, as determined from the solution of the equation for times up to the interval in question. The solution in any interval is given by a suitable modification of the zero-order solution (11), and the solution is continued from interval to interval by identifying the initial conditions of one interval with the terminal conditions of the preceding interval. Such a method will be referred to as zero-order continuation, and, while always applicable, has the disadvantage of requiring a large number of steps for an extended range.

To reduce the number of steps required, the gravitational acceleration over any interval of time can be replaced by a linear approximation whose constants are determined by the solution up to the interval. The most advantageous approximation is the quasilinear. The initial conditions for any interval are again taken as the computed terminal conditions of the preceding interval. Such a method of solution will be referred to as linear continuation.

For simplicity, let the motion be plane with an initial point O_o on the surface of the equivalent sphere S_e, and let the components of $\underset{\sim}{b}$ be measured parallel to the axes x,z of the frame O_o. Let the total range, 0 to t_n of t, be divided into n intervals, t_{k-1} to t_k $(k = 1, \ldots, n)$ with $t_o = 0$. The computed terminal point O_{k-1} in the $(k - 1)$-th interval determines a frame $x_{(k)}$, $z_{(k)}$ with parameters R_{k-1}, Θ_{k-1} for the k-th interval, as in Fig. 1 $(\Theta_o = 0)$.

theta (cap.)

In the frame O_{k-1} (which is introduced for computational convenience), the theory of the preceding sections for the frame O_o can be applied to define the pertinent parameters g_{k-1}, ω_{k-1}, $\underset{\sim}{A}_{k-1}$ by interchange of subscripts. If $\underset{\sim}{B}_{k-1}$ designates the direction-cosine matrix

omega

$$\underset{\sim}{B}_{k-1} = \begin{bmatrix} \cos\Theta_{k-1} & \sin\Theta_{k-1} \\ -\sin\Theta_{k-1} & \cos\Theta_{k-1} \end{bmatrix}, \qquad (49)$$

the g-correction equation in the k-th interval when referred to the O_{k-1} frame is

$$\begin{Bmatrix} \ddot{x}_{(k)} \\ \ddot{z}_{(k)} \end{Bmatrix} + \omega^2_{k-1}\underset{\sim}{A}_{k-1}\begin{Bmatrix} x_{(k)} \\ z_{(k)} \end{Bmatrix} = \underset{\sim}{\bar{B}}_{k-1}\begin{Bmatrix} b_x \\ b_z \end{Bmatrix} - \begin{Bmatrix} 0 \\ g_{k-1} \end{Bmatrix}, \qquad (50)$$

where $\underset{\sim}{\bar{B}}_{k-1}$ is the transpose of $\underset{\sim}{B}_{k-1}$. The formulation (50) corresponds to the use of a quasilinear approximation, which reduces to a linearized or spherical approximation in the special cases

$$\underset{\sim}{A}_{k-1} = \begin{bmatrix} 1 & 0 \\ 0 & -2 \end{bmatrix}, \qquad \underset{\sim}{A}_{k-1} = \begin{bmatrix} 1 & 0 \\ 0 & 1 \end{bmatrix}, \qquad (51)$$

respectively. The g-correction equation in the k-th interval is then

$$\begin{Bmatrix} \ddot{x} \\ \ddot{z} \end{Bmatrix} + \omega^2_{k-1}\underset{\sim}{B}_{k-1}\underset{\sim}{A}_{k-1}\underset{\sim}{\bar{B}}_{k-1}\begin{Bmatrix} x \\ z \end{Bmatrix} = \begin{Bmatrix} b_x \\ b_z \end{Bmatrix} - \underset{\sim}{B}_{k-1}\begin{Bmatrix} 0 \\ g_{k-1} \end{Bmatrix} \qquad (52)$$

when referred to the O_o frame.

In practice, it is found that linear continuation yields a considerable reduction in number of intervals as compared with zero-order continuation for the same terminal error. This fact appears by comparison of solutions I and II with

TABLE I solution III in Table I, which shows the results of three different continuation solutions carried out for the A10 trajectory. Solution I was based on the use of

rho quasilinear approximations in the intervals (as specified in Fig. 3) where $\rho \sim R_o$; comparison of the results with those of solution II brings out the superiority of the quasilinear over the linearized approximation under this condition. In carrying out these computations, the $\underset{\sim}{b}$-function (Fig. 4) was tabulated to four decimal places (after round-off) in units of g_e from the assumed trajectory (consisting of segments of analytic curves). Checks indicated that the rounding-

delta off process in $\underset{\sim}{b}$ introduced an error $|\delta \underset{\sim}{r}|$ which amounted to < 3 mi. for the solutions of Table I, which shows that the entries in the table for $|\delta \underset{\sim}{r}|$ are significant for comparison of the approximations to $\underset{\sim}{g}$.

It should be emphasized that the computations yielding Table I are of academic nature, due to neglect of the latitude-dependent component of $\underset{\sim}{g}$ and of the centrifugal and Coriolis terms in the kinetic reaction of the g-correction equation. The sum of the first two of these acceleration terms varies over a range of 0.005 g_e from the equator to the pole on the earth's surface. The systematic errors due to neglect of the variation of these terms on the A10 trajectory have been calculated approximately by a perturbation method for the case when the plane of motion coincides with the earth's equatorial plane (the error is then in this plane likewise). In this case the effect of variation of centrifugal reaction ($|\delta \underset{\sim}{r}| \sim 30$ mi.) and of Coriolis reaction ($|\delta \underset{\sim}{r}| \sim 700$ mi.) is extreme. These errors are larger by orders of magnitude than the upper limit ($|\delta \underset{\sim}{r}| < 3$ mi.) to the round-off error found above for the data of Table I. Hence, the method of computation leading to Table I, in the particular form used, has only a limited practical validity for the A10 trajectory (except as an approximation in the roughly constant plane of motion for a trajectory in the neighborhood of a pole, where the Coriolis deflection is transverse).

It is clear from these considerations that the step solution in linear continuation must be modified on trajectories of extended range, in general, to include terms corresponding to the variation of the latitude-dependent component of $\underset{\sim}{g}$, the variation of the centrifugal reaction, and the Coriolis reaction. The fact that these terms are considerably smaller than the main radial term of $\underset{\sim}{g}$ materially simplifies the problem, which will not be attempted here because of the detail involved.

The advantage of linear continuation over numerical methods such as the Runge-Kutta process consists in the fact that the length of step or the integration interval is fixed by the variation of the slowly varying $\underset{\sim}{g}$-function. From such error bounds as (22) or (31), one can estimate the number of steps required for a given terminal accuracy. In methods of the Runge-Kutta type, however, the integration interval is fixed by the variation of the rapidly varying $\underset{\sim}{b}$-term, and the possible interval is considerably smaller. Linear continuation yields a reasonable compromise between the conflicting demands of a small number of steps and simplicity of the step solution.

In conclusion the authors wish to acknowledge many helpful discussions of this problem with Dr. W. C. Randels of Northrop Aircraft Corp., Dr. R. Isaacs of The RAND Corp., and Prof. T. Dantzig of the RAND consulting staff. Thanks are due also to Mrs. M. Irving and Mrs. J. Griffith for the computational work.

TABLE I: RESULTS OF CONTINUATION SOLUTIONS .

delta

Solution	Step Solution	Number of Steps	Error $\lvert\delta \underset{\sim}{r}\rvert$ (mi.)
I	Linearized and quasilinear*	5	20
II	Linearized	39	46
III	Zero-order	39	254

* As specified in Fig. 3.

LIST OF FIGURES

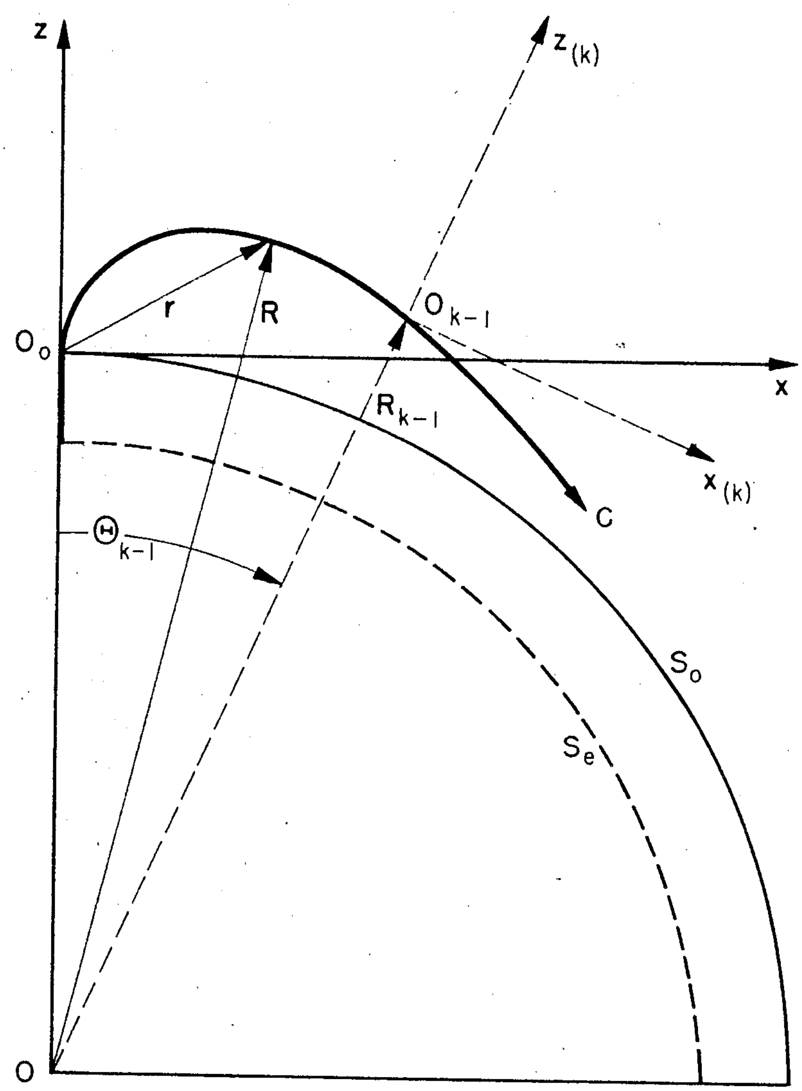

FIG.1

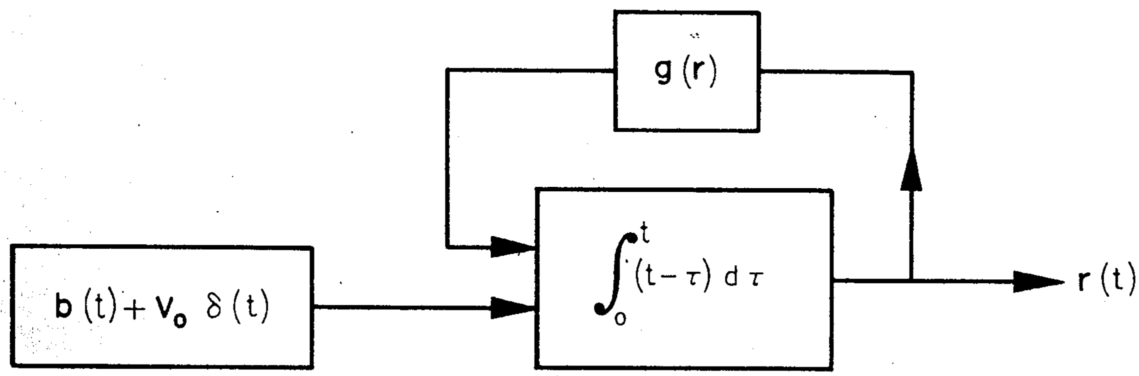

FIG. 2

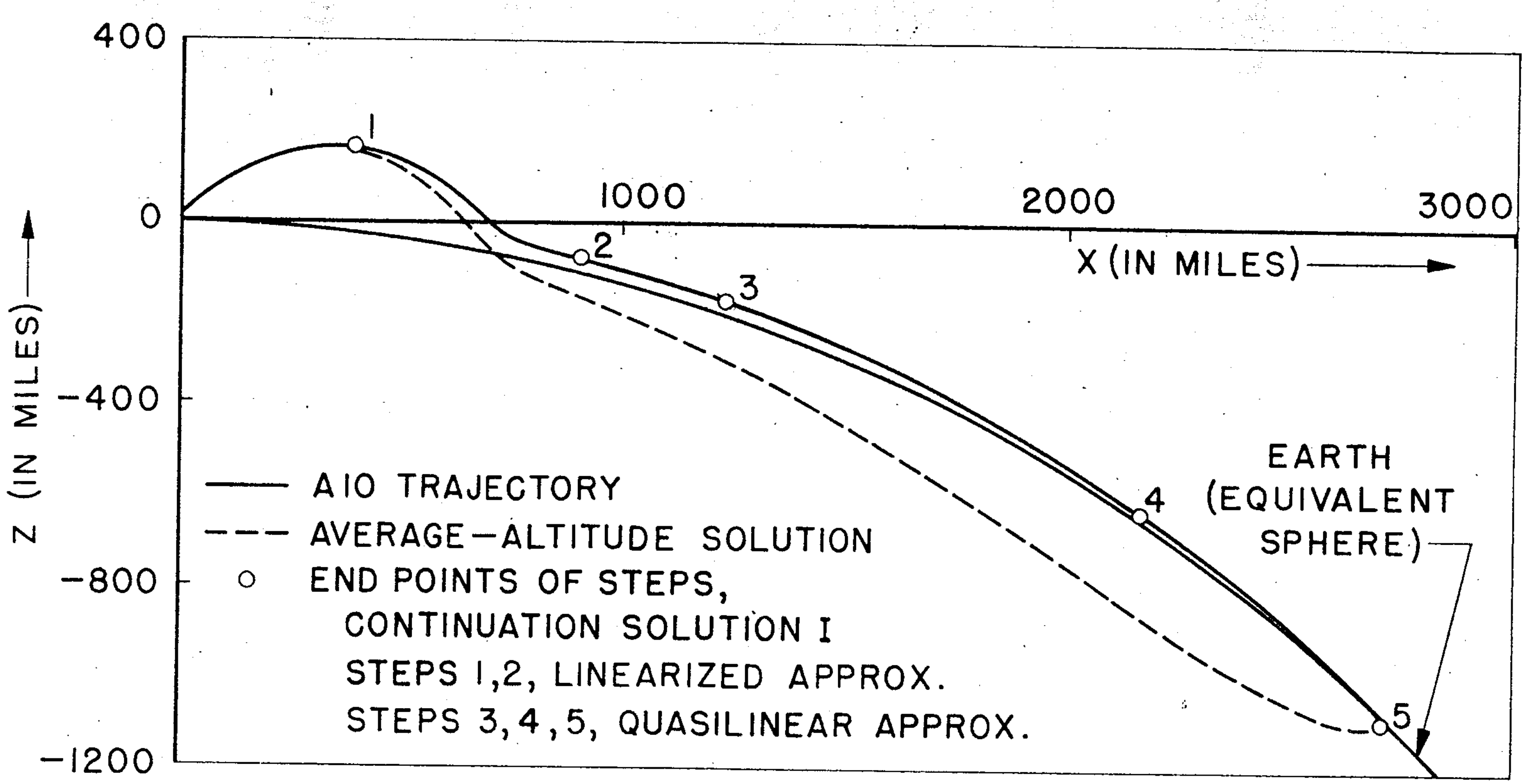
400
0
-400
-800
-1200
Z (IN MILES)
1000
2000
3000
X (IN MILES)
1
2
3
4
5
EARTH
(EQUIVALENT
SPHERE)
A10 TRAJECTORY
AVERAGE-ALTITUDE SOLUTION
END POINTS OF STEPS,
CONTINUATION SOLUTION I
STEPS 1,2, LINEARIZED APPROX.
STEPS 3,4,5, QUASILINEAR APPROX.

FIG. 3

P-121-3

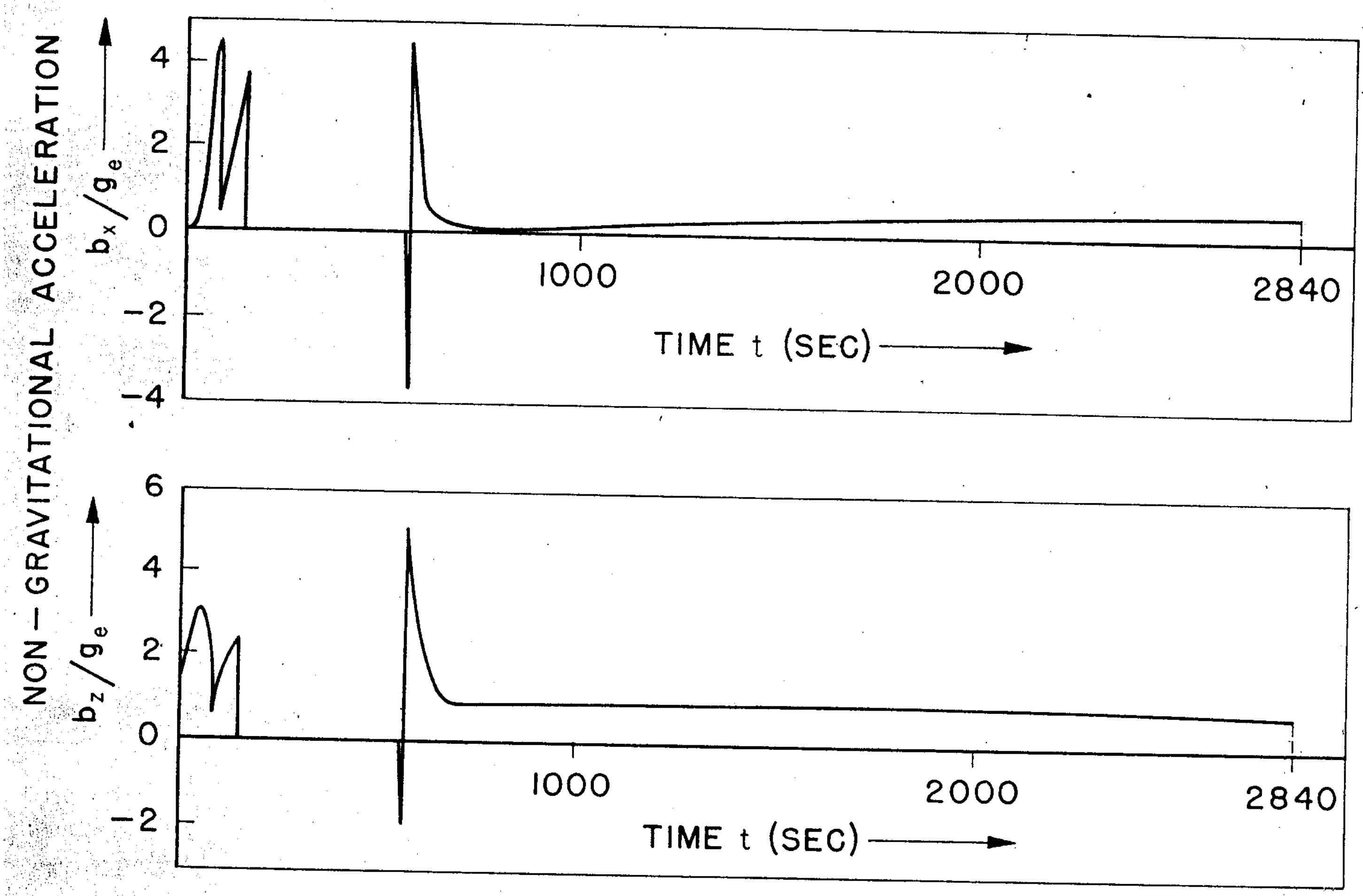
NON – GRAVITATIONAL ACCELERATION
b_x/g_e
4
2
0
-2
-4
1000
2000
2840
TIME t (SEC)
b_z/g_e
6
4
2
0
-2
1000
2000
2840
TIME t (SEC)

FIG. 4

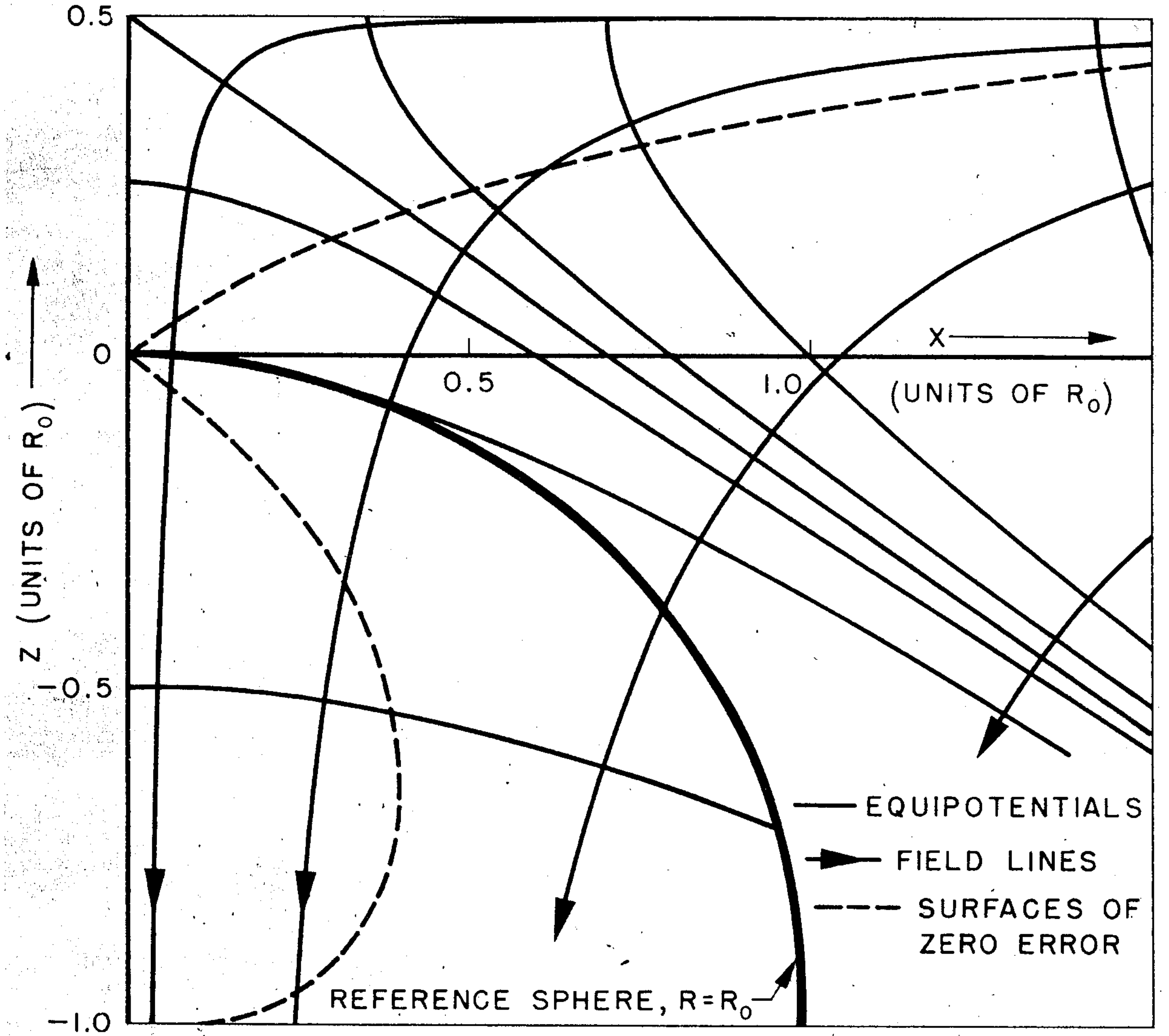

0.5
0
−0.5
−1.0
0.5
1.0
X
(UNITS OF R_0)
Z (UNITS OF R_0)
EQUIPOTENTIALS
FIELD LINES
SURFACES OF ZERO ERROR
REFERENCE SPHERE, $R=R_0$

FIG. 5

P-121-5

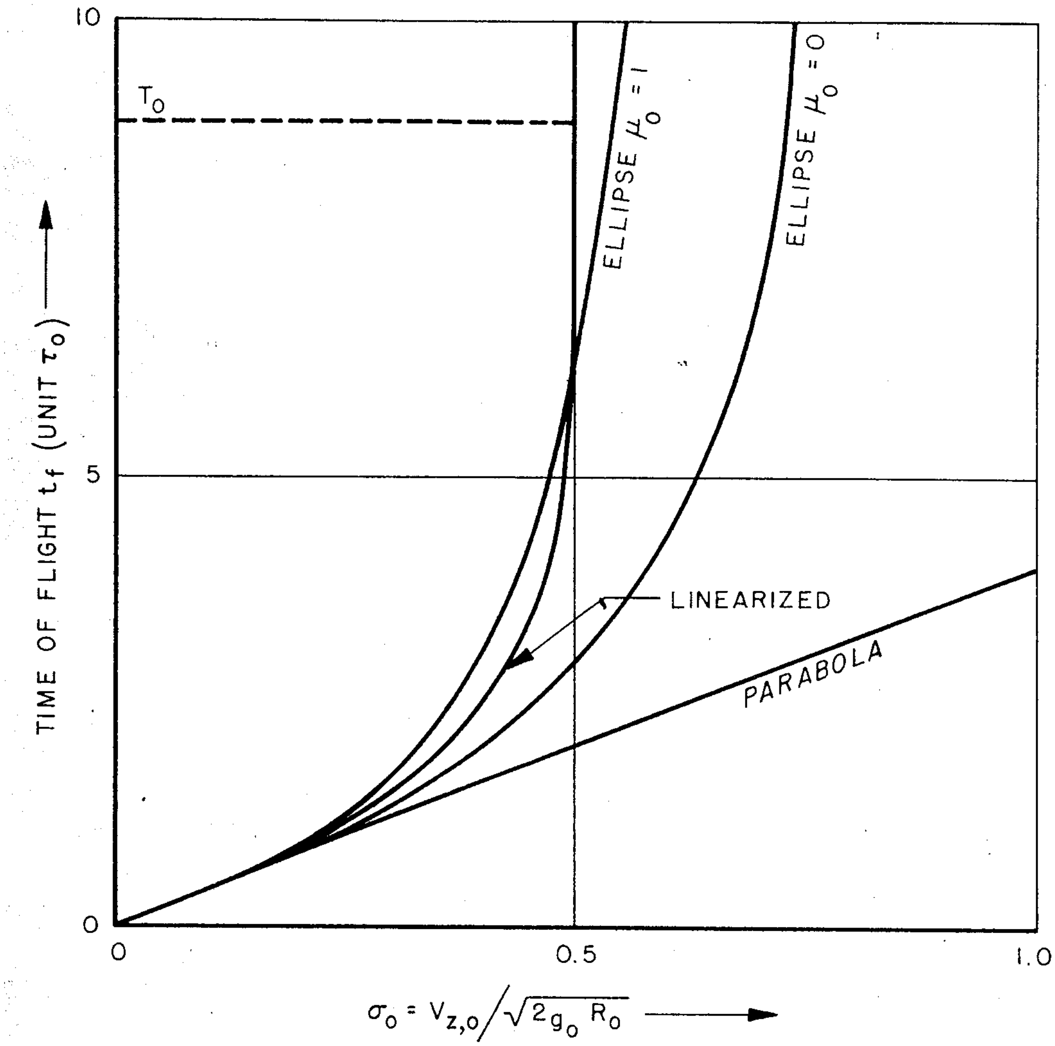

10
T_0
5
0
0
0.5
1.0
TIME OF FLIGHT t_f (UNIT τ_0)
$\sigma_0 = V_{z,o} / \sqrt{2 g_o R_o}$
ELLIPSE $\mu_0 = 1$
ELLIPSE $\mu_0 = 0$
LINEARIZED
PARABOLA

IG. 6

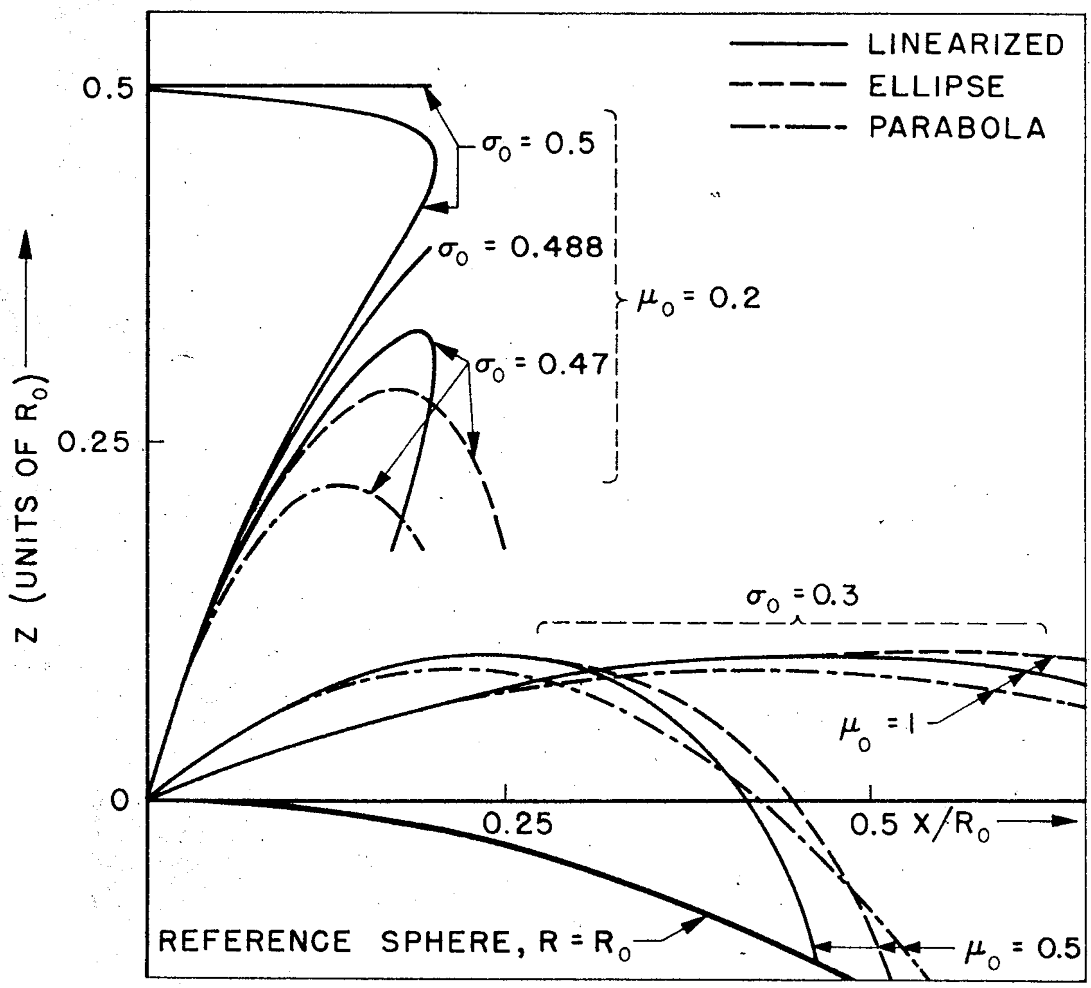

LINEARIZED
ELLIPSE
PARABOLA
0.5
0.25
0
Z (UNITS OF R_0)
σ_0 = 0.5
σ_0 = 0.488
μ_0 = 0.2
σ_0 = 0.47
σ_0 = 0.3
μ_0 = 1
0.25
0.5 X/R_0
REFERENCE SPHERE, R = R_0
μ_0 = 0.5

FIG. 7

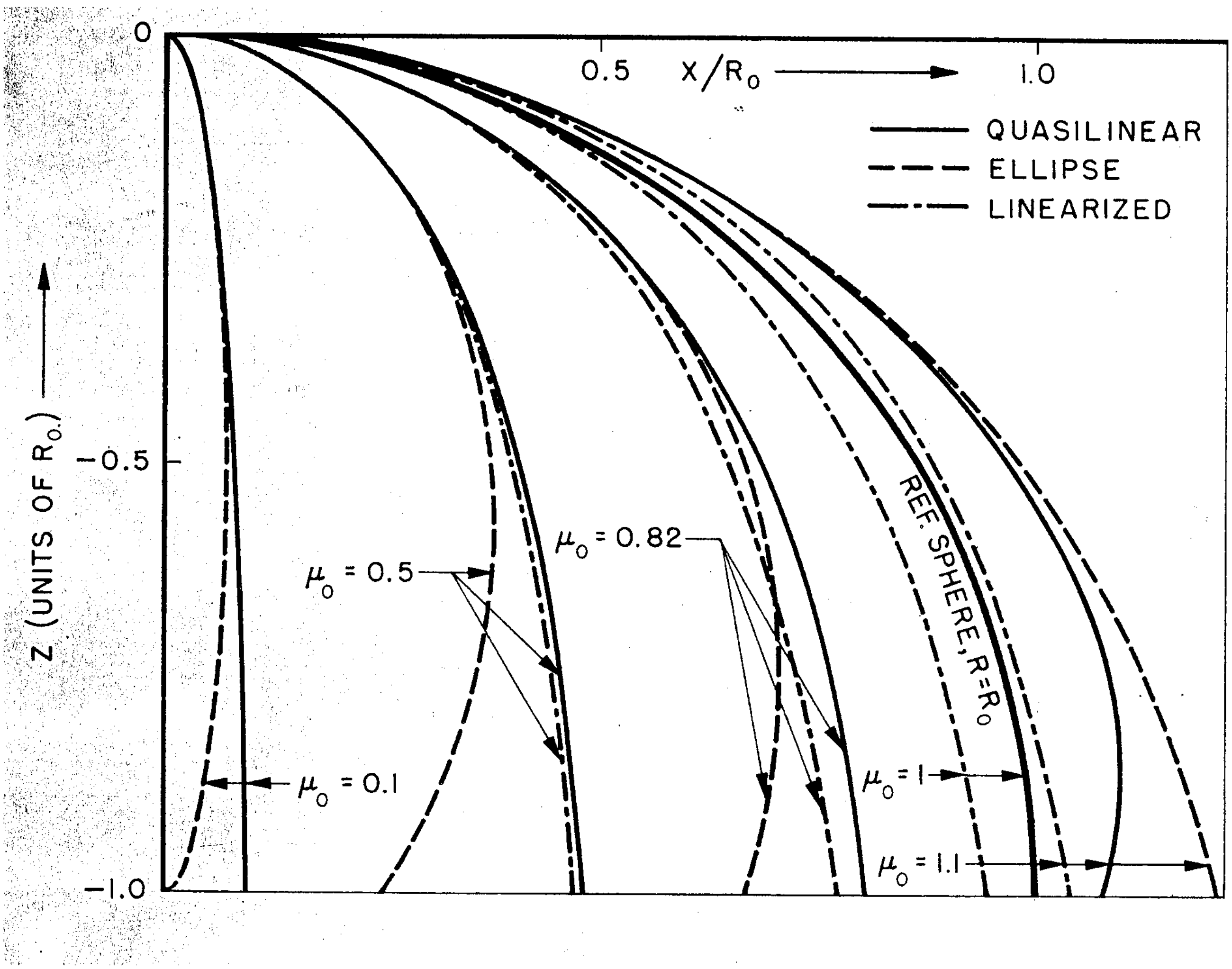

0
0.5
X/R₀
1.0
QUASILINEAR
ELLIPSE
LINEARIZED
Z (UNITS OF R₀)
−0.5
−1.0
μ_0 = 0.5
μ_0 = 0.82
μ_0 = 0.1
REF. SPHERE, R=R₀
μ_0 = 1
μ_0 = 1.1